Impact of electric quadrupolar coupling on the optical response of an array of nano-objects

2010 J. Phys.: Condens. Matter 22 225301

(http://iopscience.iop.org/0953-8984/22/22/225301)

IOP Publishing Journal of Physics: Condensed Matter

J. Phys.: Condens. Matter **22** (2010) 225301 (6pp) doi:10.1088/0953-8984/22/22/225301

Impact of electric quadrupolar coupling on the optical response of an array of nano-objects

Chien Y Lin[1], Yun H Wang[1], Jung Y Huang[1], Yongjun Liu[2] and Yiping Zhao[2]

[1] Department of Photonics and Institute of Electro-Optical Engineering, Chiao Tung University, Hsinchu 300, Taiwan, Republic of China

[2] Department of Physics and Astronomy, University of Georgia, Athens, GA 30602, USA

E-mail: jyhuang@faculty.nctu.edu.tw

Received 23 December 2009, in final form 14 April 2010
Published 20 May 2010
Online at stacks.iop.org/JPhysCM/22/225301

Abstract

Intra- and inter-particle coupling effects are important but have not been properly taken into account in modeling the optical response of an array of nano-objects. In this paper, we present a method to analyze the impact of electric quadrupolar coupling on the optical response of a layer of silver nanorods fabricated with oblique-angle deposition (OAD). Our technique can render the non-locally coupled nano-objects into an array of coarse-grained induced charges. The retrieved polarizability tensor of the silver nanorods exhibits non-zero off-diagonal components, revealing information about the array structure and inter-particle quadrupolar couplings. Thus, a more transparent picture of the correlation between the function and structure of an optical metamaterial can be yielded.

(Some figures in this article are in colour only in the electronic version)

1. Introduction

Artificial materials formed by nano-objects with appropriate shapes and morphologies can offer useful optical properties for a variety of applications ranging from sensing [1–7] to photonics [8, 9]. Among the artificial materials, arrays of nanorods with high packing density can yield large optical anisotropy or produce high optical response via couplings to surface plasmon polaritons [8]. By using these artificial materials, a variety of new functionalities including nanometer-scale polarization conversion [8], sub-wavelength imaging [10] and cylindrical superparticles with linearly polarized emission [11] have been demonstrated. To facilitate the design of an appropriate metamaterial, researchers usually relied on the Maxwell–Garnett theory to evaluate the optical response of the optical metamaterial [12, 13]. In the past, only the dipolar coupling effect has been taken into account, owing to the dimensions of the nano-objects encountered being much smaller than the optical wavelength used. However, it was found that models including only dipolar coupling may not be appropriate to describe the optical property of a single metallic nanorod with high aspect ratio [14]. Kullock *et al* [8] had also pointed out that high-order couplings could be critical in an array of nano-objects.

In this paper, we present a method to analyze the optical response of an array of nano-objects, which can render the non-locally coupled nano-objects into an array of coarse-grained induced charges. Our technique is useful not only for the design of a nanostructure with specific properties but also to yield a more intuitive and transparent picture of the correlation between the function and the structure of the metamaterial used.

Oblique-angle deposition (OAD) belongs to a physical vapor deposition process in which the incident vapor atoms are deposited on a substrate at a large incident angle with respect to the surface normal of the substrate [15]. OAD had been demonstrated to be effective, while inexpensive, for the fabrication of metallic nanorod arrays. More importantly, the size, shape and tilt angle of the nanorods can be easily controlled by adjusting the deposition parameters [16].

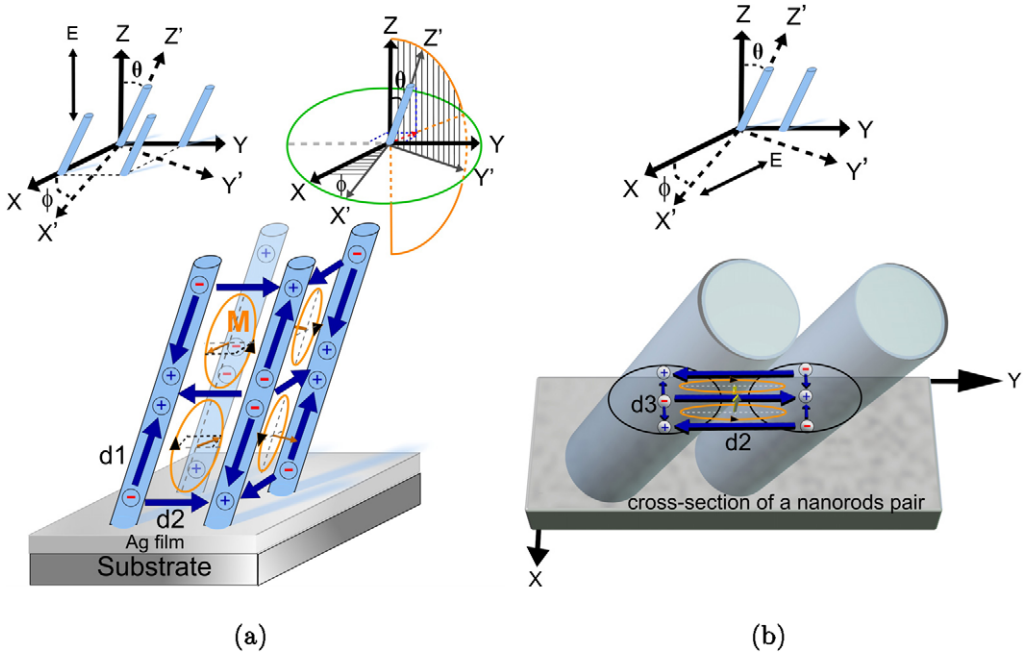

Figure 1. Schematic diagram showing the induced charge distribution on nanorods with an asymmetric distortion by an incident light field (a) along the long principal axis of the nanorods and (b) perpendicular to the nanorods. The blue-coloured arrows and '+' and '−' signs denote the induced dipole moments and charges respectively. The yellow-coloured arrows indicate the directions of magnetic dipoles, which is perpendicular to the current loop. Notice that the magnetic dipoles formed by two neighboring nanorods are antiparallel to each other. Insets describe the relative orientation of the coordinate systems of laboratory and nanorods.

Therefore, OAD has been employed for many new applications in biosensing [1–5]. Multilayer OAD has also been invoked to produce a gradient profile of refractive index for antireflection coating over a broad spectral range [15]. In view of the potential applications, we applied our method to analyze the optical responses of OAD substrates. In our case, the dimensions of the tilted silver nanorods are comparable to the incident wavelength where high-order couplings are not negligible. Our method yielded an effective polarizability tensor with non-zero off-diagonal components, revealing information about the array structure and inter-particle quadrupolar coupling effects.

2. Theoretical analysis of light scattering from a nanorod array with high packing density

An optical field $\vec{E}$ incident on an array of nanorods can induce two kinds of electric polarizations with symmetric and asymmetric excitation patterns. An in-phase current distribution produces an electric dipole ($\vec{P}$) that generates the symmetric excitation mode. The asymmetric mode originates from an electric quadrupole ($\overleftrightarrow{Q}$) and a magnetic dipole ($\vec{M}$). To depict the optical response of the array, we express the electric displacement vector $\vec{D}$ as a multipole expansion:

$$\partial_t \vec{D} = \partial_t \vec{E} + 4\pi(\partial_t \vec{P} + c\nabla \times \vec{M} - \partial_t \nabla \cdot \overleftrightarrow{Q} + \cdots). \quad (1)$$

The electrons in a dense array of nano-objects with dimensions comparable to the optical wavelength can experience different optical field strengths, depending on the coordinates of the electrons in the nano-object, array structure and optical excitation geometry. By utilizing the coarse-grain scheme, we can decompose the distorted charge distribution induced in a nano-object into a set of domains. Inside each domain, the optical field strength can be considered to be constant. Therefore, the induced charge distribution is effectively averaged to form a set of coarse-grained charged particles. The higher-order multipoles can then be viewed as a group of locally coupled coarse-grained charges. The spatial symmetry of the array structure is also automatically embedded into the strengths of the multipoles. This approach not only serves as the foundation for the discrete dipole approximation but also offers an intuitive way to look at equation (1).

Recently, Cho *et al* [17] had investigated a layer of nanorods with the discrete dipole approximation and discovered higher-order multipoles to be much weaker than the coherent sum of $\vec{P}$ and $\overleftrightarrow{Q}$. The dimensions of the nanorods are much smaller than the optical wavelength, thus only one single stack of dipoles was included in their model. Based on their finding, we considered the optical response of our film up to electric quadrupolar couplings. However, because our OAD substrates consist of an array of nanorods with dimensions comparable to the optical wavelength, we had taken into account not only the electric quadrupolar couplings in the array plane but also along the longitudinal axes of the nanorods. The resulting coarse-grain picture of electric quadrupolar couplings is complicated, with a variety of three-dimensional configurations, but can be properly depicted in figures 1(a) and (b).

We can express the total electrostatic energy of the system as $W_{\text{total}} = W_{\text{charge}} + W_{\text{dipole}} + W_{\text{q}} + \cdots$ with a quadrupolar

coupling energy of [18]

$$W_{\mathrm{q}} = -\frac{1}{6}\sum_{\alpha}\sum_{\beta} Q_{\alpha\beta}(\partial_{\alpha}E_{\beta}) \propto -\frac{L_{\alpha}L_{\beta}}{\lambda}E. \qquad (2)$$

Here L_{α} (L_{β}) denotes the separation of two neighboring induced charges along the α (β) axis of the nanorod coordinate system. In figure 1, the distance between two neighboring induced charges along the longitudinal axis of a nanorod is indicated by $d1$, the charge separation across two neighboring nanorods by $d2$ and that between induced charges confined in the cross section of a nanorod by $d3$. With the length parameters, the quadrupolar coupling energy generated by a Z-polarized light (see figure 1(a)) can be expressed as $W_{\mathrm{q},Z} = (W_{Q31} + W_{Q32} + W_{Q33}) = (2 + d1/d2)W_{Q31}$, while that induced by X- (see figure 1(b)) and Y-polarized optical field is $W_{\mathrm{q},X} = W_{\mathrm{q},Y} = (W_{Q11} + W_{Q12}) = (1 + d3/d2)W_{Q12}$.

The magnetic field radiated by a magnetic dipole $\vec{M}$ can be calculated with [18]

$$H_M = -\frac{\mathrm{i}ck^3\mathrm{e}^{\mathrm{i}kr}}{24\pi r}\hat{e}_{\alpha} \times \vec{Q}_{\alpha}, \qquad (3)$$

where $\vec{Q}_{\alpha} = \sum_{\beta} Q_{\alpha\beta}\hat{e}_{\beta}$ and $\hat{e}_{\alpha}$ is the unit vector along the α axis of the nanorod's coordinate system. The direction of $\vec{M}$, which is determined by $\hat{e}_{\alpha} \times \vec{Q}_{\alpha}(\hat{e}_{\alpha})$, is perpendicular to the current loop according to the right-hand rule. The opposite current flows shown in figures 1(a) and (b) reduce the magnetic dipole, making $\vec{M}$ to be negligible. Therefore, we can define an effective polarizability $\overleftrightarrow{\alpha}_r(\omega)$:

$$\vec{P}_r(\omega) = \vec{P} - \nabla\cdot\overleftrightarrow{Q} = [\overleftrightarrow{\alpha}_{\mathrm{P}}(\omega) - \mathrm{i}k\,\overleftrightarrow{\alpha}_{\mathrm{Q}}(\omega)\nabla]\cdot\vec{E}_0 = \overleftrightarrow{\alpha}_r(\omega)\cdot\vec{E}_0 \qquad (4)$$

to account for the electric multipoles optically induced in the nanorod array. The effective polarizability can be cast into a matrix form of

$$\overleftrightarrow{\alpha}_r = \begin{bmatrix} \alpha_{r11} & \alpha_{r12} & \alpha_{r13} \\ \alpha_{r21} & \alpha_{r22} & \alpha_{r23} \\ \alpha_{r31} & \alpha_{r32} & \alpha_{r33} \end{bmatrix}, \qquad \text{where}$$

$$\begin{aligned}
\alpha_{r11} &= \alpha_{p11} - \mathrm{i}(2\alpha_{Q11}k_x\partial_x + \alpha_{Q12}k_y\partial_y + \alpha_{Q13}k_z\partial_z),\\
\alpha_{r12} &= -\mathrm{i}\alpha_{Q12}k_x\partial_y, \qquad \alpha_{r13} = -\mathrm{i}\alpha_{Q13}k_x\partial_z,\\
\alpha_{r21} &= -\mathrm{i}\alpha_{Q21}k_y\partial_x,\\
\alpha_{r22} &= \alpha_{p22} - \mathrm{i}(2\alpha_{Q22}k_y\partial_y + \alpha_{Q21}k_x\partial_x + \alpha_{Q23}k_z\partial_z),\\
\alpha_{r23} &= -\mathrm{i}\alpha_{Q23}k_y\partial_z, \qquad \alpha_{r31} = -\mathrm{i}\alpha_{Q31}k_z\partial_x,\\
\alpha_{r32} &= -\mathrm{i}\alpha_{Q32}k_z\partial_y,\\
\alpha_{r33} &= \alpha_{p33} - \mathrm{i}(2\alpha_{Q33}k_z\partial_z + \alpha_{Q31}k_x\partial_x + \alpha_{Q32}k_y\partial_y).
\end{aligned} \qquad (5)$$

Here α_{rij} denotes a charge distortion along the j direction induced by an i-polarized incident light. In the simplest case, the polarizability tensor shall have a diagonal matrix form, implying that the electric dipole components of a nanorod can only be induced by an optical field along the same direction of the dipole components. However, due to inter-rod couplings, an electric polarization induced by an optical field component perpendicular to the electric polarization is not negligible, leading to nonvanishing off-diagonal components of $\overleftrightarrow{\alpha}_r(\omega)$. The inset in figure 1 shows the relative orientation of the coordinate systems (X, Y, Z) and (X', Y', Z'), denoting the coordinate systems of the laboratory and the array, respectively. For an array with a square lattice, an optical field along the X' or Y' direction induces only an electric quadrupole in the X'–Y' plane. Therefore, both α_{Q13} and α_{Q23} shall vanish. For nanorods with cylindrical symmetry, $\alpha_{Q11} = \alpha_{Q22}$ and $\alpha_{Q12} = \alpha_{Q21}$.

We can conduct the coordinate transformation from (X, Y, Z) to (X', Y', Z') with the Z' axis along the long axis of the nanorods by using

$$\overleftrightarrow{T} = \begin{bmatrix} \cos\phi & \sin\phi & 0 \\ -\cos\theta\sin\phi & \cos\theta\cos\phi & -\sin\theta \\ -\sin\theta\sin\phi & \sin\theta\cos\phi & \cos\theta \end{bmatrix}. \qquad (6)$$

Here θ and ϕ denote the angles between the Z and Z' axes and the X and X' axes, respectively. Therefore, the incident optical field in the coordinate system of the nanorods can be calculated by

$$\vec{E}' = \begin{bmatrix} E'_{X'} \\ E'_{Y'} \\ E'_{Z'} \end{bmatrix} = \overleftrightarrow{T}\cdot\vec{E}. \qquad (7)$$

The light scattering intensity from the nanorod array thus becomes

$$I_{\mathrm{scatt}} = I_i|\hat{e}_{\mathrm{s}}\,\overleftrightarrow{T}^{-1}\cdot\overleftrightarrow{\alpha}_r\cdot\overleftrightarrow{T}\,\hat{e}_{\mathrm{i}}|^2, \qquad (8)$$

where $\hat{e}_{\mathrm{i}}$ and $\hat{e}_{\mathrm{s}}$ are the unit vectors of the incident and the scattering fields in the laboratory coordinate system.

To yield further insight into the optical response of the nanorod array, we discuss a connection of the dielectric permittivity (ε) and magnetic permeability (μ) of the layer with the effective polarizability of the coarse-grained particles. As mentioned above, the multiple stack geometry of coarse-grained charges could effectively suppress the axial-vector-like magnetic dipole. This leads to the optical response of the nanorod array to be mainly contributed from the electric dipole and quadrupole. Because of the sub-wavelength-scale inhomogeneity of the medium, optical wave propagation inside the system becomes spatially dispersive and a non-zero local field can only exist with specific k^2, which is a solution of the characteristic equation directly from Maxwell's equations. Based on the formalism developed by Cho *et al* [17], the electric quadrupole $\overleftrightarrow{\alpha}_{\mathrm{Q}}$ can contribute to a magnetic permeability $\mu^{-1} = 1 - 4\pi(\omega/c)^2\,\overleftrightarrow{\alpha}_{\mathrm{Q}}$, while the dielectric permittivity of the film is given by $\varepsilon = 1 + 4\pi\,\overleftrightarrow{\alpha}_{\mathrm{P}}$. The effective polarizabilities $\overleftrightarrow{\alpha}_{\mathrm{P}}$ and $\overleftrightarrow{\alpha}_{\mathrm{Q}}$ of the quasiparticles can be experimentally determined by light scattering as shown by equation (8).

3. Experimental details of light scattering measurement

We prepared tilted Ag nanorods on glass substrates by using the oblique-angle vapor deposition method as detailed by Zhao *et al* [19]. These films consist of a layer of 20 nm Ti and 500 nm Ag films, and an array of tilted silver nanorods with

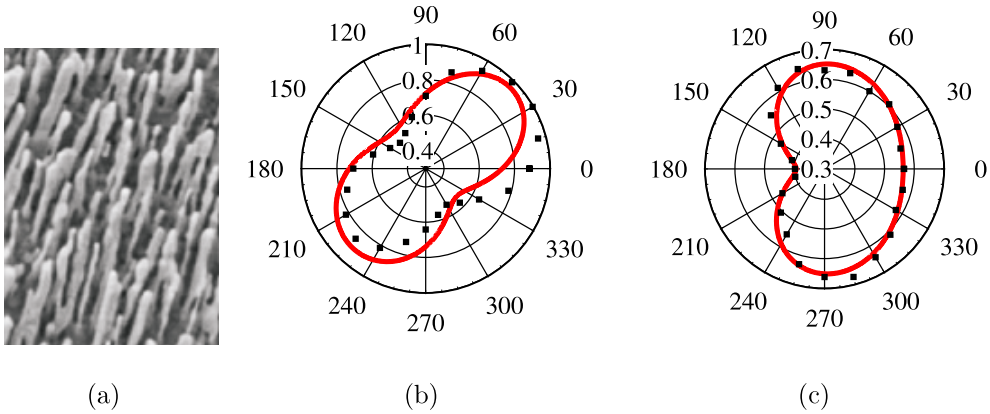

Figure 2. (a) SEM image of an OAD Ag nanorod substrate. (b) The azimuthal patterns of the light scattering from tilted Ag nanorods were measured (filled squares). The zero azimuthal angle implies the tilt plane of the silver nanorods to be along the incident plane of the excitation light. The fittings to equation (8) are presented by red solid curves. The p-polarized scattering light was measured with s-polarized incident light. (c) Both of the excitation and scattering fields are p-polarized.

an average length of 900 nm, average diameter of 100 nm and average spacing of 177 nm [19]. Figure 2(a) shows an SEM image of a typical OAD film. Those Ag nanorods had an average tilting angle of 73° with respect to the surface normal of the substrate [20].

For light scattering measurements, a continuous wave (CW) laser with a wavelength of 532 nm was used to excite an OAD substrate. We aligned the polarization of the laser beam to be perpendicular to the incident plane (s-polarized) and then controlled its polarization with a Pockels cell driven at a half-wave voltage of 3.5 kV. This enables the polarization of the incident optical field to be switched easily from s- to p-polarized.

We set the incident angle of the excitation beam at 45° to maximize the light scattering intensity according to the finding reported in the literature [21]. We used a microscope objective lens to collect the scattering signal along the substrate normal and analyzed the scattering signal with a polarizer. The resulting optical signal was detected with a photomultiplier tube.

4. Results and discussion

To retrieve the effective polarizability tensor of a silver nanorod in an OAD film, we measured the optical scattering signal from the OAD film as a function of azimuthal angle ϕ of the substrate. The inclined plane of the nanorod is defined to be the plane formed by the major Z' axis of the nanorod and the substrate normal, while the incident plane contains the incident beam and the substrate normal. The azimuthal angle ϕ is defined to be zero as the inclined plane is aligned with the incident plane. When the polarization vector of the incident or the scattering light is perpendicular to the incident plane, it is indicated as s-polarized, whereas p-polarized is used when the polarization of the incident or the scattering field lies in the incident plane. Figures 2(b) and (c) show the azimuthal patterns of the p-polarized scattering signal from silver nanorods excited by s- and p-polarized light, respectively.

By fitting the two azimuthal patterns to equation (8), the polarizability tensor of the tilted silver nanorods averaged over the illuminated area can be deduced. Without including $\overleftrightarrow{\alpha}_{\mathrm{Q}}\, k^2$ a good fit cannot be obtained. We also need an isotropic term to yield a satisfactory fit, suggesting that in our OAD film the underlying Ag thin film and the Ag nanorod arrays (see figure 1(a)) are coupled together and contribute to the observed optical response. A satisfactory fitting, shown as the solid curves in figures 2(b) and (c), yields the following polarizability tensor:

$$\overleftrightarrow{\alpha}_r = \begin{bmatrix} \alpha_{r11} & \alpha_{r12} & \alpha_{r13} \\ \alpha_{r21} & \alpha_{r22} & \alpha_{r23} \\ \alpha_{r31} & \alpha_{r32} & \alpha_{r33} \end{bmatrix} = V \begin{bmatrix} 5.10 & -0.24 & 0 \\ -0.24 & 5.10 & 0 \\ 5.52 & 2.42 & 15.29 \end{bmatrix}. \tag{9}$$

We found that α_{r31} is about twice as large as α_{r32}, indicating that our OAD nanorod array deviates significantly from a square lattice that requires $\alpha_{r31} = \alpha_{r32}$. The deviation shall originate from the lack of positional order in the OAD array.

As indicated by equation (4), we can decompose $\overleftrightarrow{\alpha}_r$ into $\overleftrightarrow{\alpha}_{\mathrm{P}}$ and $\overleftrightarrow{\alpha}_{\mathrm{Q}}$ as

$$\overleftrightarrow{\alpha}_{\mathrm{P}} = \begin{bmatrix} \alpha_{P11} & 0 & 0 \\ 0 & \alpha_{P11} & 0 \\ 0 & 0 & \alpha_{P33} \end{bmatrix} = V \begin{bmatrix} 0.90 & 0 & 0 \\ 0 & 0.90 & 0 \\ 0 & 0 & 1.15 \end{bmatrix}, \tag{10}$$

$$\overleftrightarrow{\alpha}_{\mathrm{Q}}\, k^2 = k^2 \begin{bmatrix} \alpha_{Q11} & \alpha_{Q12} & \alpha_{Q13} \\ \alpha_{Q12} & \alpha_{Q11} & \alpha_{Q23} \\ \alpha_{Q31} & \alpha_{Q31} & \alpha_{Q33} \end{bmatrix} = V \begin{bmatrix} -2.22 & 0.24 & 0 \\ 0.24 & -2.22 & 0 \\ -5.52 & -2.42 & -3.10 \end{bmatrix}, \tag{11}$$

where V is the average volume of coarse-grained quasiparticles. As expected, the X' and Y' components of $\overleftrightarrow{\alpha}_{\mathrm{P}}$ are smaller than those along the Z' axis for a prolate ellipsoidal nanoobject [22]. From the ratio of the induced dipolar components, we found that each 900 nm long silver nanorod with a diameter of 100 nm is optically driven to produce about seven coupled dipoles along the longitudinal direction. Therefore, the result

clearly supports our view on the nanorod array as a thin layer containing multiple stacks of induced dipoles.

The term of $\overleftrightarrow{\alpha}_Q\, k^2$ originates from the electric quadrupolar couplings in the OAD array of silver nanorods. As the inter-rod coupling is not negligible, the new principal axes (X'', Y'', Z'') of the polarizability tensor have different orientations from the coordinate system of nanorods (X', Y', Z'). By diagonalizing the polarizability tensor, the new principal axes can be yielded. The eigenvalues were found to be $(\alpha_{r11} - \alpha_{r12}, \alpha_{r11} + \alpha_{r12}, \alpha_{r33})$, corresponding to the principal axes (X'', Y'', Z''), respectively. We found that the in-plane coupling causes a rotation with an angle of $\tan^{-1}(\alpha_{r12}/\alpha_{r21})$ in the X'–Y' plane. A non-zero α_{r31} leads to a tilt of the X'' axis from X' by an angle of $\cos^{-1}[\alpha_{r31}/\sqrt{\alpha_{r31}^2 + (\alpha_{r11} - \alpha_{r12} - \alpha_{r33})^2/2}]$. A similar result was also found with a non-zero α_{r32}.

When the dimension of a single silver nanorod is greater than the mean free path of electrons in silver (∼57 nm), the size effect of the dielectric constant is insignificant [23]. Assuming the OAD nanorod array embedded in air, we estimated the resulting dielectric constant to be $1.487 + 0.015\mathrm{i}$. The real part of the effective dielectric constant of our OAD silver nanorod array is much larger than the imaginary part, indicating that the real part of the dielectric constant dominates the optical response and justifies the real-valued results of equations (10) and (11).

The intra- and inter-rod electric quadrupolar couplings have a contribution to the effective magnetic permeability of the layer. In our nanorod array, there are N quadrupolar units per unit volume with $N \gg 1$, so the effective magnetic permeability of the film can be deduced to be

$$\mu = \frac{1}{NV}\begin{bmatrix} 0.036 & 0.004 & 0 \\ 0.004 & 0.036 & 0 \\ -0.068 & -0.035 & 0.026 \end{bmatrix}. \qquad (12)$$

The non-local coupling effect has a significant influence on the optical response of the nanorod array. At this wavelength, while the diagonal terms of the magnetic permeability remain positive as expected, the off-diagonal components α_{r31} and α_{r32} become negative.

Recent research on optical cloaking devices or omnidirectional retroreflectors used highly ordered array structures to enable new optical functionality [24] or yield a profile of refractive index [25]. The non-local coupling effects in a nanorod array can expand the design of new photonic devices by utilizing the concept of transformation optics [26]. The quadrupolar coupling strength, decreasing with inter-rod distance as r^{-5} [27], allows us to engineer a proper lattice structure to increase α_{r12}. In addition, an increase in the aspect ratio of nanorods shall lead to increased stacks of induced dipoles. Therefore, by properly tuning the distance between two neighboring nanorods and the length of the nanorod, one shall be able to engineer an appropriate metamaterial structure with a specific optical property.

5. Conclusion

We presented a method to analyze the optical response of a metamaterial formed by a dense array of nano-objects. Our technique can render the non-locally coupled nano-objects into an array of coarse-grained induced charges. We applied the method to investigate a layer of tilted silver nanorods fabricated with the oblique-angle deposition (OAD) technique. The retrieved effective polarizability tensor of the tilted silver nanorods was found to possess non-zero off-diagonal terms, indicating that the intra- and inter-rod electric quadrupolar couplings cannot be neglected. The electric quadrupolar polarizability plays the major role in determining the effective magnetic permeability, which results in some of the off-diagonal terms being negative. Our method could be used to provide extra degrees of freedom for the development of new meso-optical devices and suggests a negative refractive metamaterial can also be formed by a carefully designed array structure.

References

[1] Shanmukh S, Jones L, Zhao Y-P, Driskell J, Tripp R and Dluhy R 2008 Identification and classification of respiratory syncytial virus (rsv) strains by surface-enhanced Raman spectroscopy and multivariate statistical techniques *Anal. Bioanal. Chem.* **390** 1551

[2] Juna Y W, Sheikholeslamia S, Hostetterb D R, Tajonb C, Craikb C S and Paul Alivisatosa A 2009 Continuous imaging of plasmon rulers in live cells reveals early-stage caspase-3 activation at the single-molecule level *Proc. Natl Acad. Sci. USA* **106** 17735

[3] Driskell J D, Seto A G, Jones L P, Jokela S, Dluhy R A, Zhao Y-P and Tripp R A 2008 Rapid microrna (mirna) detection and classification via surface-enhanced Raman spectroscopy (sers) *Biosens. Bioelectron.* **24** 923

[4] Chu S-Y, Huang Y-W and Zhao Y-P 2008 Silver nanorod arrays as a surface-enhanced Raman scattering substrate for foodborne pathogenic bacteria detection *Appl. Spectrosc.* **62** 922

[5] Driskell J D, Shanmukh S, Liu Y-J, Hennigan S, Jones L, Zhao Y-P, Dluhy R A, Krause D C and Tripp R A 2008 Infectious agent detection with sers-active silver nanorod arrays prepared by oblique angle deposition *IEEE Sensors J.* **8** 863

[6] Stewart M, Anderton C, Thompson L, Maria J, Gray S, Rogers J and Nuzzo R 2008 Nanostructured plasmonic sensors *Chem. Rev.* **108** 494

[7] Aslan K, Lakowicz J R and Geddes C D 2005 Plasmon light scattering in biology and medicine: new sensing approaches, visions and perspectives *Curr. Opin. Chem. Biol.* **9** 538

[8] Kullock R, Hendren W R, Hille A, Grafstrom S, Evans P R, Pollard R J, Atkinson R and Eng L M 2008 Polarization conversion through collective surface plasmons in metallic nanorod arrays *Opt. Express* **16** 21671

[9] Kwon M-K, Kim J-Y, Kim B-H, Park I-K, Cho C-Y, Byeon C C and Park S-J 2008 Surface-plasmon-enhanced light-emitting diodes *Adv. Mater.* **20** 1253

[10] Ono A, Kato J I and Kawata S 2005 Subwavelength optical imaging through a metallic nanorod array *Phys. Rev. Lett.* **95** 267407

[11] Zhuang J, Shaller A D, Lynch J, Wu H, Chen O, Li A D Q and Charles Cao Y 2009 Cylindrical superparticles from semiconductor nanorods *J. Am. Chem. Soc.* **131** 6084

[12] García-Vidal F J, Pitarke J M and Pendry J B 1997 Effective medium theory of the optical properties of aligned carbon nanotubes *Phys. Rev. Lett.* **78** 4289

[13] Atkinson R, Hendren W R, Wurtz G A, Dickson W, Zayats A V, Evans P and Pollard R J 2006 Anisotropic optical properties of arrays of gold nanorods embedded in alumina *Phys. Rev.* B **73** 235402

[14] Bryant G W, de Abajo F J G and Aizpurua J 2008 Mapping the plasmon resonances of metallic nanoantennas *Nano Lett.* **8** 631–6
[15] Kuo M L, Poxson D J, Kim Y S, Mont F W, Kim J K, Schubert E F and Lin S Y 2008 Realization of a near-perfect antireflection coating for silicon solar energy utilization *Opt. Lett.* **33** 2527
[16] Abelmann L and Lodder C 1997 Oblique evaporation and surface diffusion *Thin Solid Films* **305** 1
[17] Cho D J, Wang F, Zhang X and Shen Y R 2008 Contribution of the electric quadrupole resonance in optical metamaterials *Phys. Rev.* B **78** 121101(R)
[18] Jackson J D 1975 *Classical Electrodynamics* (New York: Wiley)
[19] Chaney S B, Shanmukh S, Duluhy R A and Zhao Y-P 2005 Aligned silver nanorod arrays produce high sensitivity surface-enhanced Raman spectroscopy substrates *Appl. Phys. Lett.* **87** 031908
[20] Zhao Y-P, Chaney S B, Shanmukh S and Dluhy R A 2006 Polarized surface enhanced Raman and absorbance spectra of aligned silver nanorod arrays *J. Phys. Chem.* B **110** 3153
[21] Liu Y, Fan J, Zhao Y-P, Shanmukh S and Dluhy R A 2006 Angle dependent surface enhanced Raman scattering obtained from an Ag nanorod array substrate *Appl. Phys. Lett.* **89** 173134
[22] Kooij E S and Poelsema B 2006 Shape and size effects in the optical properties of metallic nanorods *Phys. Chem. Chem. Phys.* **8** 3349
[23] Dienerowitz M, Mazilu M and Dholakia K 2008 Optical manipulation of nanoparticles: a review *J. Nanophoton.* **2** 021875
[24] Gabrielli L H, Cardenas J, Poitras C B and Lipson M 2009 Silicon nanostructure cloak operating at optical frequencies *Nat. Photon.* **3** 461
[25] Ma Y G, Ong C K, Tyc T and Leonhardt U 2009 An omnidirectional retroreflector based on the transmutation of dielectric singularities *Nat. Mater.* **8** 639
[26] Leonhardt U and Philbin T G 2009 Transformation optics and the geometry of light *Prog. Opt.* **53** 69–152
[27] Klimov V V and Ducloy M 2005 Quadrupole transitions near an interface: general theory and application to an atom inside a planar cavity *Phys. Rev.* A **72** 043809